

Mobility-enhanced signal response in metapopulation networks of coupled oscillators

CHUANSHENG SHEN^{1,2}, HANSHUANG CHEN³ and ZHONGHUAI HOU² ^(a)

¹ *Hefei National Laboratory for Physical Sciences at Microscales & Department of Chemical Physics, University of Science and Technology of China, Hefei, 230026, China*

² *Department of Physics, Anqing Normal University, Anqing, 246011, China*

³ *School of Physics and Material Science, Anhui University, Hefei, 230039, China*

PACS 89.75.Hc – Networks and genealogical trees

PACS 05.45.Xt – Synchronization; coupled oscillators

PACS 89.75.Fb – Structures and organization in complex systems

Abstract – We investigate the effect of mobility on the response of coupled oscillators to a sub-threshold external signal in metapopulation networks, wherein each node represents a subpopulation with overdamped bistable oscillators that can randomly diffuse between nodes. With increasing mobility rate, the oscillators undergo transitions from intrawell to interwell motion, demonstrating clearly mobility-enhanced signal amplification. Moreover, the response shows non-monotonic dependence on the mobility rate, i.e., a maximal gain occurs at a moderate level of mobility. This interesting phenomenon is robust against variations in the overall density, network size, as well as network topology. In addition, a simple mean-field analysis is carried out to qualitatively illustrate the simulation results.

Introduction. – Enhancing the collective response to a weak input signal is an important and challenging problem in a variety of fields, not only in that of traditional signal processing but also in those such as particle physics [1], gravitational wave search [2], and medical science [3,4]. Many natural and artificial information-processing systems are connected together to form functional networks and spontaneously adjust their internal machinery to enhance the sensitivity to external signals. For instance, cells and microorganisms respond to changes in external environment by means of an interconnected network of receptors, messengers, protein kinases and other signaling molecules [5–7]. One of the most intriguing part of these phenomena was amplified signal response. It has been shown that random fluctuations can enhance the response to weak periodic driving, as observed in many different physical, chemical and biological scenarios [8–10]. Recently, amplified signal response in complex network of coupled oscillators has drawn considerable attention [7, 11–16]. It has been found that the weak external signals can be amplified by the heterogeneity in degree of the network [7, 11, 12], adaptive coupling weights between

the signal node and its neighbors [13], neuronal diversity on complex networks [14] and a multilayer feedforward network [15]. A one-body theory which gave analytic expressions of the gain and the degree of the unit with the maximum response to the input signal in terms of the coupling strength was also developed [16].

Nevertheless, previous studies on signal response in complex networks only deal with the case of immobile elements and each network node is occupied by one single element. Very recently, the metapopulation network model [17], which incorporates subpopulation in the node, mobility over the nodes, and a complex network topology, has attracted much attention. This model has been successfully exploited in different contexts, such as epidemic spreading [18–20], biological pattern formation [21, 22], chemical reactions [23], population evolution [24], and many other spatially distributed systems [25, 26]. It is shown that the mobility and the density of the individuals could have drastic impact on the emergence of collective behaviors in general [17, 27], and particularly, mobility induced and tuned synchronization of coupled oscillators have been reported [28–30]. Therefore, one may ask: How would the mobility influence the signal response in metapopulation networks of coupled oscillators?

^(a) hzh1j@ustc.edu.cn

In the present work, we consider a metapopulation networked system wherein each node is occupied by any number of overdamped bistable oscillators, subject to a sub-threshold external signal. By stochastic simulations of the involved dynamical reaction-diffusion processes, we find that, the signal response exhibits a clear-cut maximum at an optimal level of mobility rate. Furthermore, we show this nontrivial phenomenon is robust to the density and network size as well as different network topologies. A simple mean-field (MF) analysis is given to help us understand the simulation results.

Model description. – We consider a system of M individuals distributed in N distinct subpopulations labeled μ , each corresponding to a network node, and assume that the number of individuals in node μ is N_μ , satisfying $\sum_{\mu=1}^N N_\mu = M$. Thus, the density ρ of the metapopulation is given by $\rho = M/N$. Individuals inside each subpopulation run through the paradigmatic bistable oscillators, and the dynamics of the i th-oscillator located in the μ th node is described by:

$$\dot{x}_i = x_i - x_i^3 + \frac{C}{N_\mu} \sum_{j \in \mu} (x_j - x_i) + A \sin(\omega t) \quad (1)$$

Here x_i ($i = 1, \dots, M$) is the state variable of the i -th unit at time t , and C is the coupling strength. A and ω are the amplitude and frequency of the external periodic forcing, respectively.

The above equation actually defines the “reaction” process that governs the overdamped motion of a Brownian particle in a double-well potential with subthreshold periodic forcing. We now assume that the particles can diffuse randomly among the nodes. The system evolves in time according to the following rules [17]. We introduce a discrete time step τ representing the fixed time scale of the process. The reaction and diffusion rates are therefore converted into probabilities. In the reaction step, all the particles are updated in parallel according to Eq.1. After that, diffusions take place by allowing each particle to move into a randomly chosen neighboring node with probability $V\tau$, where V denotes the mobility rate. If not otherwise specified, the parameters are $N = 1000$, $\tau = 0.001$ and $C = 0.005$. We choose the mobility rate V as the main control parameter. Each simulation plot is obtained via averaging over 50 independent runs.

Simulation results. – To begin, we consider scale-free networks generated by using the Barabási–Albert (BA) model [31] with power-law degree distribution $p(k) \sim k^{-3}$ and average degree $\langle k \rangle = 6$. We fix $\rho = 10$ and vary V to investigate how the state variables of oscillators evolve in time. Initially, the oscillators are randomly distributed among the nodes and homogeneously assigned the initial position at ± 1 , which are the two minima of the double-well potential. The signal is considered to be subthreshold, i.e., it does not suffice to induce the oscillators to jump between the two minima in the absence of

diffusion. For small V , the oscillators are separated into two distinct subsets: Some oscillate around the minimum 1 and the others around -1, depending on their initial conditions. As examples, typical time series of $x_i(t)$ for several randomly-chosen oscillators are plotted in Fig.1(I) for $V = 2.5 \times 10^{-5}$. For moderate mobility rate $V = 2.5 \times 10^{-3}$ as shown in Fig.1(II), jumps between the two stable wells tend to occur periodically in time, driven by the periodic force. However, for large V , say $V = 0.25$ in Fig.1(III), the oscillators are synchronized but all confined into one single well. Therefore, we observe interesting mobility-induced transitions from intrawell to interwell motion, and then to synchronized single-well motion. We note that the final state for large V may depend on the amplitude or the frequency of the external signal. For instance, for $A = 0.38$ ($\omega = 0.015$), the transition from intrawell to internal well motion still occurs when V increases from small values, but the oscillators finally oscillate separately around the two minima if V is large enough(not shown). We also note that this nontrivial transition and re-entrance phenomenon is observed if one fix V and let ρ change. In this latter case, the oscillators will remain in the well they initially are no matter how large ρ is.

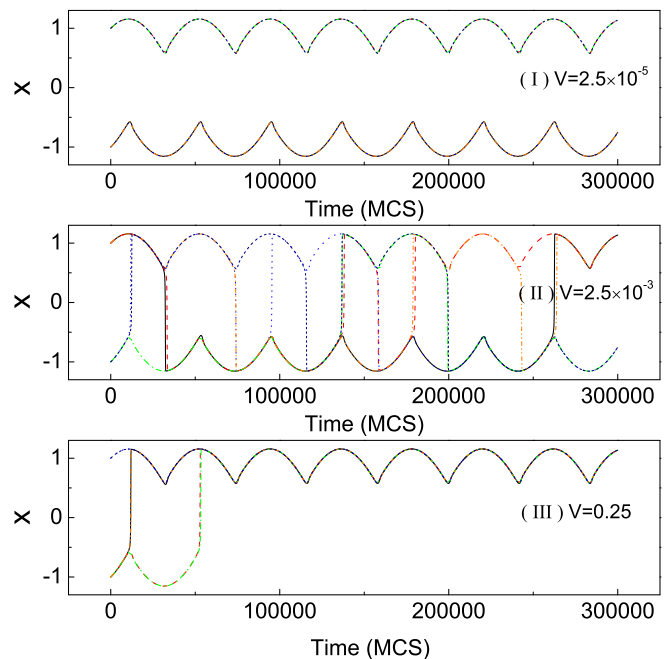


Fig. 1: (Color online) Typical time evolutions of the state variables $x_i(t)$ for several randomly-chosen oscillators at $V = 2.5 \times 10^{-5}$ (upper panel), $V = 2.5 \times 10^{-3}$ (middle panel) and $V = 0.25$ (lower panel). Time in the simulations is measured in units of Monte Carlo steps (MCS), where one MCS is defined as M reaction and diffusion attempts, M being the number of the total oscillators in the metapopulation network. It is shown that the time series undergo mobility-induced transitions from intrawell to interwell motion, and then to synchronized single-well motion. Other parameters are $N = 200$, $\langle k \rangle = 6$, $\rho = 10$, $A = 0.39$ and $\omega = 0.015$.

To quantitatively measure the signal response, we introduce a gain factor G which is defined as follows [7, 13, 16],

$$G = \left[\frac{1}{AM} \sum_{i=1}^M (\max x_i - \min x_i) / 2 \right], \quad (2)$$

where $[\cdot]$ stands for averaging over 50 different network realizations for each value of V . Clearly, a large G means a larger signal response. Figs.2 plot the G as a function of V for fixed $\rho = 10$ with varying signal amplitude A or frequency ω . Clearly, G shows a nonmonotonic dependence on the mobility rate as expected from Fig.1. Note that for large V , the final stationary values of G may have two different values depending on ω and A in a somewhat complicated way: One approaches 1.5 for small ω and large A , as depicted by red solid circles and dark yellow dotted circles in Fig.2(a) and (b), and the other approaches 0.75 for small ω with small A , or for relatively large ω , as also shown in Fig.2. The time series shown in Fig.1 correspond to different mobility rates indicated by the three arrows in Fig.2(b): The transitions from intrawell to interwell and then to synchronized single-well motion are demonstrated.

So far, the results are all for scale-free coupled networks. One may wonder whether the above interesting findings are sensitive to the network topology or not. Thus, we have also performed similar studies on other types of networks, such as small world networks and random networks. Fig.3 plots the dependences of G on V for a typical small-world network and a random network, shown by triangles and squares respectively. Apparently, the qualitative behaviors are the same as those observed for scale-free networks. The only difference is that the optimal mobility rate for the maximal signal response is different.

Mean field analysis. – To get more insight into the aforementioned results, here we present a simple mean-field analysis by considering a model system consisting of only two nodes. This makes the problem mathematically tractable, while still capable of capturing the main trait of mobility. Assuming that the node 1 and 2 hold N_1 and N_2 oscillators respectively, we can introduce the average state variables $X_1 = \frac{1}{N_1} \sum_{i \in 1} x_i$ and $X_2 = \frac{1}{N_2} \sum_{j \in 2} x_j$, whose dynamics is governed by the following equations via averaging Eq. (1) over each subpopulation,

$$\dot{X}_1 = X_1 - \frac{1}{N_1} \sum_{i \in 1} x_i^3 + A \sin(\omega t) + V(X_2 - X_1) \quad (3a)$$

$$\dot{X}_2 = X_2 - \frac{1}{N_2} \sum_{j \in 2} x_j^3 + A \sin(\omega t) + V(X_1 - X_2) \quad (3b)$$

The first three terms in the right-hand side of Eq. (3a) account for averages with respect to the counterparts in the Eq.(1), and the last term represents the diffusion of elements into and out of the node 1. Note here that we have chosen the characteristic time τ as the discrete time step to integrate Eq.(1). Equation (3b) can be interpreted in a similar manner. Following the scheme

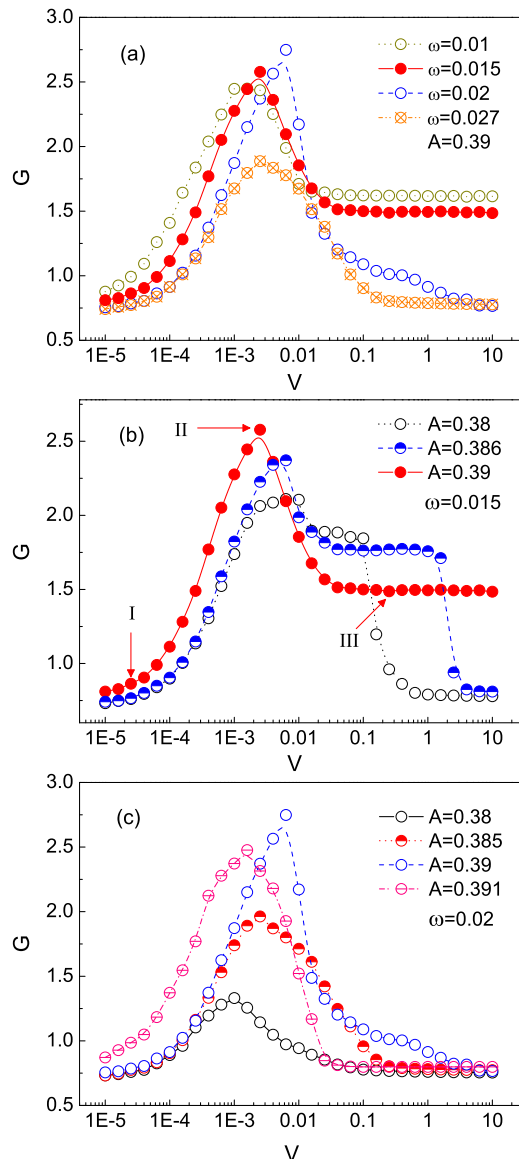


Fig. 2: (Color online) The gain factor G as a function of mobility rate V on BA scale-free networks at different ω for fixed $A = 0.39$ (a), (b) and (c) corresponding to different A at fixed $\omega = 0.015$ and $\omega = 0.02$ respectively. The representative time evolutions at different mobility rates indicated by arrows in panel (b) are shown in Fig.1.

used in Ref. [32], one may introduce the variances of state variables within the node 1 and node 2, denoted by $\sigma_1 = \frac{1}{N_1} \sum_{i \in 1} (x_i - X_1)^2$ and $\sigma_2 = \frac{1}{N_2} \sum_{j \in 2} (x_j - X_2)^2$ respectively. Assuming these variances to satisfy Gaussian distribution, Eqs. (3) become

$$\dot{X}_{1,2} = X_{1,2}(1 - 3\sigma_{1,2}) - X_{1,2}^3 + A \sin(\omega t) + V(X_{2,1} - X_{1,2}) \quad (4)$$

However, this equation is yet not solvable analytically since we do not know the exact expressions of $\sigma_{1,2}$. To proceed, we numerically calculate $\sigma_{1,2}$ by using an ensemble average along with the numerical integration of Eq.(4).

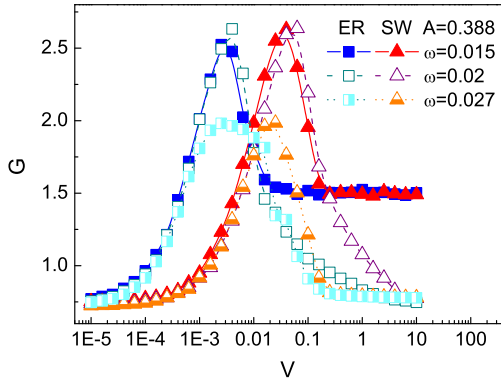


Fig. 3: (Color online) The gain factor G as a function of mobility rate V in the metapopulation model, triangles and squares correspond to small-world network and random network respectively, both on a synthesized 1000-node network with $\langle k \rangle = 6$.

The gain factor associated with this simple model is then obtained as $G = \frac{1}{2A} \sum_{i=1}^2 (\max X_i - \min X_i)/2$. In Fig.4, we give the results of G as a function of the mobility rate V for the two-node network, where the lines denote the results obtained from Eq.(4) and the symbols from Eq. (1). Clearly, the mean field equation (4) can reproduce qualitatively well the main character: There exists an optimal mobility rate where the gain reaches the maximum.

Discussion and conclusion. – It is now well known that mobility may play constructive roles in many coupled systems. For example, mobility can lead to the optimal synchronization in two-dimensional coupled phase oscillator model [33] and partially occupied networks [34], tune synchronization of integrate-and-fire oscillators [30], influence the synchronization pathway in metapopulations of mobile agents [29] and affect the epidemic threshold in metapopulation networks [35], *etc.* Our findings here show that natural systems might profit from their mobility in order to optimize the response to an external stimulus. Recently, we have also found that mobility can considerably induce metapopulation coupled oscillators undergoing phase transitions from incoherent to amplitude death, and then to synchronized state [36]. Such constructive effects of mobility in complex systems may deserve more and more attention in future works.

In summary, we have studied the signal response of coupled bistable oscillators in metapopulation networks, wherein different subpopulations are connected by fluxes of individuals. By extensive numerical simulations, we show that the mobility plays nontrivial roles on the collective response of the system, by demonstrating an interesting type of mobility-enhanced signal response to an external periodic forcing, which is robust to the density, network size as well as network topology. We have also performed a simple mean field analysis which can qualitatively reproduce the simulation results. Since many real-world networks, such as cellular networks, protein

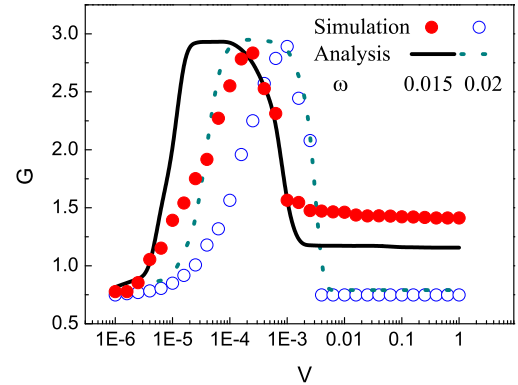


Fig. 4: (Color online) The gain factor G as a function of mobility rate V on two-node networks. The lines denote theoretical results and the symbols denote simulation ones. Other parameters are $A = 0.388$ and $\rho = 200$.

networks, gene networks, and so on, inevitably involve variances in the mobility, and their collective dynamics could be modeled by coupled oscillators, these results may find many applications in several fields of physics, neuroscience, and biology. Our study may provide valuable insights into the mobility-induced collective response to the external signals that take place in other metapopulation networked systems.

This work was supported by the National Natural Science Foundation of China (Grants No. 21125313, No. 20933006, No. 91027012, and No. 11205002). C.S.S. was also supported by the Key Scientific Research Fund of Anhui Provincial Education Department (Grant No.KJ2012A189).

REFERENCES

- [1] ASZTALOS S. J., CAROSI G., HAGMANN C., KINION D., VAN BIBBER K., HOTZ M., ROSENBERG L. J., RYBKA G., HOSKINS J., HWANG J., SIKIVIE P., TANNER D. B., BRADLEY R. and CLARKE J., *Phys. Rev. Lett.*, **104** (2010) 041301.
- [2] SESANA A., HAARDT F., MADAU P. and VOLONTERI M., *Astrophys. J.*, **623** (2005) 23.
- [3] CONTI M., *IEEE Trans. Nucl. Sci.*, **53** (2006) 1188.
- [4] ICHIKI A. and TADOKORO Y., *Phys. Rev. E*, **87** (2013) 012124.
- [5] BRAY D., *J. Theor. Biol.*, **143** (1990) 215.
- [6] ALON U., *Science*, **301** (2003) 1866.
- [7] ACEBRÓN J. A., LOZANO S. and ARENAS A., *Phys. Rev. Lett.*, **99** (2007) 128701.
- [8] GAMMAITONI L., HÄNGGI P., JUNG P. and MARCHESONI F., *Rev. Mod. Phys.*, **70** (1998) 223.
- [9] GAO Z., HU B. and HU G., *Phys. Rev. E*, **65** (2001) 016209.
- [10] LINDNER B., GARCÍA-OJALVO J., NEIMAN A. and SCHIMANSKY-GEIER L., *Phys. Rep.*, **392** (2004) 321.

- [11] PERC M., *Phys. Rev. E*, **78** (2008) 036105.
- [12] LIU Z. and MUNAKATA T., *Phys. Rev. E*, **78** (2008) 046111.
- [13] ZHOU J., ZHOU Y. and LIU Z., *Phys. Rev. E*, **83** (2011) 046107.
- [14] SHEN C., CHEN H. and ZHANG J., *Chin. Phys. Lett.*, **25** (2008) 1591.
- [15] LIANG X., ZHAO L. and LIU Z., *IEEE Trans. Neural Netw.*, **23** (2012) 1506.
- [16] KONDO T., LIU Z. and MUNAKATA T., *Phys. Rev. E*, **81** (2010) 041115.
- [17] COLIZZA V., PASTOR-SATORRAS R. and VESPIGNANI A., *Nat. Phys.*, **3** (2007) 276.
- [18] GAUTREAU A., BARRAT A. and BARTHÉLEMY M., *J. Theor. Biol.*, **251** (2008) 509.
- [19] BARONCHELLI A., CATANZARO M. and PASTOR-SATORRAS R., *Phys. Rev. E*, **78** (2008) 016111.
- [20] MELONI S., PERRA N., ARENAS A., GÓMEZ S., MORENO Y. and VESPIGNANI A., *Scientific Reports*, **1** (2011) 62.
- [21] KONDO S. and MIURA T., *Science*, **329** (2010) 1616.
- [22] NAKAMASU A., TAKAHASHI G., KANBE A. and KONDO S., *Proc. Natl. Acad. Sci. U.S.A.*, **106** (2009) 8429.
- [23] NAKAO H. and MIKHAILOV A. S., *Nat. Phys.*, **6** (2010) 544.
- [24] BALCAN D. and VESPIGNANI A., *J. Theor. Biol.*, **293** (2012) 87.
- [25] BARTHÉLEMY M., *Phys. Rep.*, **499** (2011) 1.
- [26] VESPIGNANI A., *Nat. Phys.*, **8** (2012) 32.
- [27] COLIZZA V. and VESPIGNANI A., *Phys. Rev. Lett.*, **99** (2007) 148701.
- [28] FUJIWARA N., KURTHS J. and DÍAZ-GUILERA A., *Phys. Rev. E*, **83** (2011) 025101(R).
- [29] GÓMEZ-GARDEÑES J., NICOSIA V., SINATRA R. and LATORA V., *arXiv:1211.4616*, (2012) .
- [30] PRIGNANO L., SAGARRA O. and DÍAZ-GUILERA A., *Phys. Rev. Lett.*, **110** (2013) 114101.
- [31] BARABÁSI A.-L. and ALBERT R., *Science*, **286** (1999) 509.
- [32] TESSONE C. J., MIRASSO C. R., TORAL R. and GUNTON J. D., *Phys. Rev. Lett.*, **97** (2006) 194101.
- [33] URIU K., ARES S., OATES A. C. and MORELLI L. G., *Phys. Biol.*, **9** (2012) 036006.
- [34] LIU Z., *Phys. Rev. E*, **81** (2010) 016110.
- [35] SHEN C., CHEN H. and HOU Z., *Phys. Rev. E*, **86** (2012) 036114.
- [36] SHEN C., CHEN H. and HOU Z., *arXiv:1302.3480*, (2013) .